2021

Solar-Powered Mechanical Subcooling Refrigeration System for Hot Climates

Sara Barghash
Kuwait University

Ammar Bahman
Kuwait University, a.bahman@ku.edu.kw

Osama Ibrahim

Solar-Powered Mechanical Subcooling Refrigeration System for Hot Climates

Sara BARGHASH, Ammar M. BAHMAN*, Osama M. IBRAHIM

Kuwait University, College of Engineering and Petroleum, Mechanical Engineering Department, Kuwait City, Kuwait
sara.barghash@ku.edu.kw; a.bahman@ku.edu.kw; osama.ibrahim@ku.edu.kw

* Corresponding Author

ABSTRACT

This study investigates the performance of a solar-powered mechanical subcooling cycle to improve the performance of a refrigeration system in hot climates. The mechanical subcooling cycle helped the main refrigeration cycle by further subcool the refrigerant and improve the cooling capacity. The mechanical subcooling cycle used the energy generated by the solar photovoltaics to run its own compressor. The system was evaluated under Kuwait's weather condition for a typical residential air conditioning (AC) unit of 5 tons of refrigeration (17.6 kW), where different refrigerants were examined in the mechanical subcooling cycle. The refrigerants considered in this study were R-410A, R-32, R-290, R-600, R-600a, R-1234yf, and R-1234ze(E). Parametric studies were performed using an equation solver software to understand the effect of the subcooling temperature and solar panel area on the overall performance of the refrigeration system. The results were compared with a baseline conventional refrigeration cycle using R-410A. The results show that the optimum subcooling temperature for the summer days in Kuwait ranges from 10°C to 20°C, while the best refrigerant that maximizes the overall performance of the system is R-600. In addition, the dedicated mechanical subcooling system improved the overall system COP between 5% up to 16% compared to the conventional system during the typical day of July which is the hottest month in Kuwait. The results also concluded that the solar panel area required to produce sufficient solar power to run the dedicated mechanical subcooling cycle is 3.9 m^2 using a single-axis solar tracking system, which saves utility power during the summer months between 17-20%.

1. INTRODUCTION

The vapor-compression cycle is the basic thermodynamic refrigeration cycle that is still used in many applications such as heating, air-conditioning, and refrigeration. The performance of such thermodynamic cycles is highly dependent on the operating indoor and outdoor temperatures. Air conditioning (AC) systems contribute significantly to energy consumption in hot climate regions. In addition to greater cooling requirements in hot climates, cooling equipment efficiency decreases with increasing outdoor temperature. Therefore, it is advantageous to utilize the available solar energy to achieve higher efficiency at high ambient conditions. Since Kuwait's climate is very hot, it is desirable to improve the performance of the basic thermodynamic cycle. To achieve better performance, several modifications can be executed on the cycle. In recent years, many publications considered the performance of air-conditioners, especially for hot climates.

Bahman et al. (2014) suggested two technologies, which are liquid flooded compression with regeneration system and vapor injected compression with the economizing system to improve the performance of AC systems in hot climate regions. The performance of both systems was studied under various ambient temperatures and using four different refrigerants, namely, R-410A, R-290, R-1234yf, and R-32. Both systems were compared with a conventional AC system to evaluate the improvements. The numerical analyses showed that the vapor injected compression system provided significant improvement on the compressor discharge temperature except for the case of using R-32 as a working refrigerant. However, the flooded system resulted in a relatively higher compressor discharge temperature. With respect to the system coefficient of performance (COP), the vapor injection technology improved the performance of the system significantly except for the case of using R-1234yf as a working refrigerant. On the other hand, the oil-flooded system showed a significant COP enhancement when using R-1234yf and negligible improvement for the other refrigerants. Koronaki et al. (2016) tested a single-stage, two-bed adsorption solar cooling system under Eastern Mediterranean conditions, specifically Athens Greece, Nicosia Cyprus, and Alexandria Egypt. The performance of the solar cooling system under investigation was examined for various cooling water inlet temperatures and multiple

solar thermal collectors. The obtained results demonstrated that the best performance of the system occurs in Nicosia, although this city has the greatest outside temperature among the studied cities. Comparing between different thermal collectors showed that glazed photovoltaic-thermal (PV/T) collectors are better than unglazed ones because they lead to better system performance. However, the results showed that the advanced flat plate solar collector is the best among all types as it improved the performance of the system with a maximum cooling capacity of 16 kW and an energy efficiency defined as the ratio between the sum of the chiller and electrical powers and the power related to irradiation of 21.7%. Bellos et al. (2017) introduced a new solar-assisted mechanical compression refrigeration system using evacuated tube collectors to minimize electricity consumption using solar energy. The proposed design was examined for different evaporation and condensation temperatures and pressure ratios. The simulation results showed that the novel design had larger COP values for higher evaporation temperatures and lower condensation temperatures. For this design, the optimum value obtained for the pressure ratio was 75% of the maximum operating pressure. Moreover, the proposed environmentally-friendly method showed excellent energy savings between 15% and 25% with a small collecting area. Li et al. (2017) introduced a vapor-compression chiller with subcooling power that is provided by a dedicated subcooling cycle to examine the ratio of the rise in the cooling output to the subcooling power under different operating conditions. To satisfy this goal, a thermodynamic model was simulated based on several assumptions, including steady-state, negligible pressure losses within the pipeline and heat exchanger, and negligible heat transfer between the system and the surroundings. The results of this work showed that the subcooling power could not be completely transformed to enlarge the cooling output. In addition, it was found that the ratio of the rise in the cooling output to the subcooling power was significantly affected by the speed of the compressor and the flow rates of cooling water and chilled water. The optimum value of the subcooling power needed to increase the ratio of the rise in the cooling output to the subcooling power was 1 kW. Li et al. (2018) examined a solar absorption-subcooled compression hybrid cooling system that has an operating principle close to that of a vapor-compression chiller with dedicated mechanical subcooling for high-rise buildings. The investigated system is a combination of an absorption subsystem defined by the characteristic equation and a compression subsystem modeled by the lumped parameter method. The proposed method is supported by a prototype and experimental work for verification. This method is advantageous because the absorption subsystem showed a good performance that resulted in a higher evaporation temperature in the absorption chiller and hence reduces energy consumption. The maximum deviation between the experimental and the theoretical results was ±4%. Additionally, the proposed hybrid system model provided credible convergence as the operating condition differs from the design condition. The results showed that the COP of both the absorption subsystem and the compression subsystem was affected by the operating conditions.

This work proposes a combined cycle in which a dedicated mechanical subcooling cycle is used in conjunction with the main cycle in order to improve the cycle's performance without increasing the energy consumption or harming the environment by utilizing the solar energy to operate the mechanical subcooling cycle. The dedicated mechanical subcooling cycle helps the main cycle by further subcooling the refrigerant leaving the condenser, and therefore more liquid refrigerant enters the evaporator so that cooling capacity can be improved. In this work, the main cycle uses R-410A as a refrigerant, whereas the solar-powered mechanical subcooling cycle examines different refrigerants to maximize the overall combined cycle performance at hot climate such as Kuwait. The study also investigates the effect of the solar panel area on the performance of the cycle during the hot months in Kuwait, as well as the utility power saved. This work introduces the suitable solar panel size and number of batteries required to run the solar-powered dedicated mechanical subcooling cycle in order to achieve the desired performance.

2. MODEL DESCRIPTION

2.1 Cycle and Refrigerant

The basic vapor-compression refrigeration cycle consists of evaporator, compressor, condenser, and expansion valve, as shown in Figure 1. It is desired to enhance the performance of this basic cycle with an environmentally-friendly method. To fulfill this goal, the basic cycle described by the lower part in Figure 1 is combined with a dedicated mechanical subcooling cycle that is driven by solar power using solar photovoltaics (PV). The solar-assisted mechanical subcooling cycle is represented by the upper part, as in Figure 1. For the system shown in Figure 1, the lower cycle uses R-410A as a working refrigerant since R-410A is the current refrigerant used in most AC applications, while the upper cycle uses the optimum refrigerant which is selected based on the criteria described in this work. The main advantage of the system described in Figure 1 is that it further subcools the refrigerant in the cycle and hence provides additional capacity. The P-h diagram for the combined cycle is shown in Figure 2. The cycle starts with the refrigerant compressed to higher pressure in the main cycle (process line 1-2). Then, the refrigerant passes through the condenser

with constant pressure as represented in the process line (2-3), where it condenses to lower temperature. From Figure 2, It is very clear that the combined cycle has a larger process line (2-3), which indicates that it provides more cooling. The process line (3-4) shown in Figure 1 represents the heat exchanger (HX) process in the lower part of the cycle where the pressure remains constant, and the condenser temperature is subcooled. The extra cooling is the reason for the subcooling of the refrigerant as the saturation temperature lines indicate in Figure 2. After that, the refrigerant is expanded in the expansion valve, having a constant enthalpy, as explained in the process line (4-5). For the upper part of the cycle shown in Figure 1, the process line (6-7) is the compression process during which the refrigerant is compressed to higher pressure in the dedicated mechanical subcooling cycle. The refrigerant is then condensed to a lower temperature with constant pressure, process line (7-8). After that, the refrigerant is expanded with a constant enthalpy in the expansion valve to lower pressure and temperature, as indicated by the process line (8-9). The process line (9-6) explains the HX process for the dedicated mechanical subcooling cycle where the pressure remains constant, and the enthalpy increases.

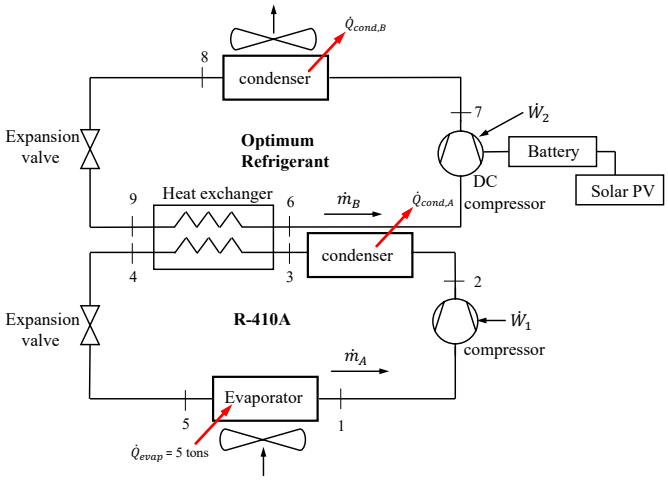

Figure 1: Schematic diagram for the solar-powered mechanical subcooling refrigeration system.

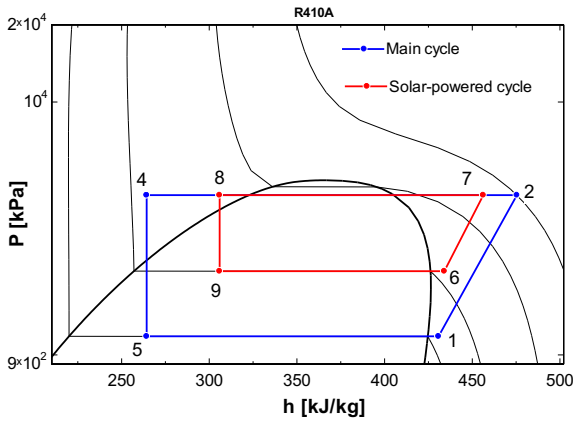

Figure 2: P-h diagram for the solar-powered mechanical subcooling system (R-410A used in both cycles).

To choose the best refrigerant to be used in the dedicated mechanical subcooling cycle, different refrigerants were examined. The tested refrigerants are R-410A, R-1234yf, R-1234ze(E), R-32, R-290, R-600 and R-600a. All these refrigerants are used in AC applications and have zero Ozone Depletion Potential (ODP). Also, all the suggested refrigerants are non-toxic except R32. R-1234yf, R-1234ze(E), R-290, R-600, and R-600a have very low (less than 8) Global Warming Potential (GWP).

2.2 Thermodynamic Analysis

2.2.1 Baseline Cycle Analysis: The basic refrigeration cycle with no subcooling (*i.e.,* baseline cycle) is modeled using the thermodynamics laws, as shown in Table 1. The subscripts in the equations are based on the numbering shown in Figure 1 noting that in the case of having the basic cycle alone, there will be four states only—State 4 on Figure 1 will be ignored, and State 5 will be considered as the fourth state—. Note that the set of equations was solved using an engineering equation solver software, EES (Klein and Alvarado, 2019). EES was also used to get the properties of the refrigerants and to perform the parametric studies.

The mass flow rate of R-410A in the baseline cycle is calculated from the cooling capacity as follows

$$\dot{m}_A = \frac{\dot{Q}_{evap}}{h_1 - h_5} \tag{1}$$

The work rate of the compressor is defined as follows

$$\dot{W}_1 = \dot{m}_A \left(h_{2a} - h_1\right) \tag{2}$$

The COP of the baseline cycle is then can be calculated from the following equation

$$\mathrm{COP}_{base} = \frac{\dot{Q}_{evap}}{\dot{W}_1} \tag{3}$$

The hourly COP of the cycle is obtained using a parametric study by varying the outdoor temperature per hour during the average day of each hot month. The outdoor temperatures used to represent the actual temperature in Kuwait at each specific time. The calculation details and assumptions of each state in the cycle are clearly represented in Table 1.

Table 1: Equations and assumptions used to model the baseline cycle at each thermodynamic state.

State 1	State 2	State 3	State 4
$T_1 = T_{evap} + T_{sh}$ $P_1 = P(T_{evap}, x_1 = 1)$ $h_1 = h(T_1, P_1)$ $s_1 = s(T_1, P_1)$	$s_{2s} = s_1$ $P_2 = P_3$ $h_{2s} = h(s_{2s}, P_2)$ $h_{2a} = h_1 + \frac{h_{2s} - h_1}{\eta_c}$ $s_{2a} = s(h_{2a}, P_2)$ $T_2 = T(h_{2a}, P_2)$	$T_3 = T_{cond} - T_{sc}$ $P_3 = P(T_{cond}, x_3 = 0)$ $h_3 = h(T_3, P_3)$ $s_3 = s(T_3, P_3)$	$P_4 = P_1$ $h_4 = h_3$ $T_4 = T(h_4, P_4)$ $s_4 = s(h_4, P_4)$

2.2.2 Combined Cycle Analysis: After analyzing the baseline cycle, the combined cycle was studied. As mentioned earlier, the refrigerant used in the baseline cycle is R-410A, while the solar-powered cycle uses the optimum selected refrigerant, as explained later in this work. When simulating the combined cycle, State 4 for the lower baseline cycle is changed to State 5. The subcooling temperature for the combined cycle is found as follows

$$T_{sc,2} = T_3 - T_4 \tag{4}$$

The mass flow rate of refrigerant in the dedicated mechanical subcooling cycle is calculated from the following formula

$$\dot{m}_B = \dot{m}_A \left(\frac{h_3 - h_4}{h_6 - h_9} \right) \tag{5}$$

Then, the work rate of the solar-powered compressor is determined as follows

$$\dot{W}_2 = \dot{m}_B (h_{7a} - h_6) \tag{6}$$

The total work rate of the combined cycle is defined as

$$\dot{W}_{combined} = \dot{W}_1 + \dot{W}_2 \tag{7}$$

The coefficient of performance of the combined cycle is then determined as follows

$$\mathrm{COP}_{combined} = \frac{\dot{Q}_{evap}}{\dot{W}_{combined}} \tag{8}$$

After that, it is important to evaluate the improvement on the COP value by comparing the COP of the combined cycle with that of the baseline cycle with no subcooling as follows

$$\mathrm{COP}_{imp} = \frac{\mathrm{COP}_{combined} - \mathrm{COP}_{base}}{\mathrm{COP}_{base}} \times 100 \tag{9}$$

The percentage of power saved by implementing the proposed cycle is obtained as follows

$$\dot{W}_{saved} = \frac{\dot{W}_{base} - \dot{W}_{combined}}{\dot{W}_{base}} \times 100 \tag{10}$$

Finally, the effectiveness of the heat exchanger can be evaluated as follows

$$\varepsilon = \frac{\Delta h_{HX}}{\Delta h_{HX,max}} \tag{11}$$

The calculation details of each state in the combined solar-powered mechanical subcooling cycle are listed, as shown in Table 2. Note that the first three states are exactly similar to that of the conventional baseline cycle.

Table 2: Equations and assumptions used to model the combined solar-powered mechanical subcooling cycle at each thermodynamic state.

State 4	State 5	State 6	State 7
$P_4 = P_3$ $h_4 = h(T_4, P_4)$ $s_4 = s(T_4, P_4)$	$P_5 = P_1$ $h_5 = h_4$ $T_5 = T(h_5, P_5)$ $s_5 = s(h_5, P_5)$	$P_6 = P_9$ $T_{sat,6} = T(P_6, x_6 = 0)$ $T_6 = T_{sat,6} + T_{sh}$ $h_6 = h(T_6, P_6)$ $s_6 = s(T_6, P_6)$	$s_{7s} = s_6$ $P_7 = P_8$ $h_{7s} = h(s_{7s}, P_7)$ $h_{7a} = h_6 + \frac{h_{7s} - h_6}{\eta_c}$ $s_{7a} = s(h_{7a}, P_7)$ $T_7 = T(h_{7a}, P_7)$
State 8	**State 9**	**Heat exchanger**	
$T_8 = T_{cond} - T_{sc}$ $P_8 = P(T_{cond}, x_8 = 0)$ $h_8 = h(T_8, P_8)$ $s_8 = s(T_8, P_8)$	$T_9 = T_4 - T_{pinch}$ $h_9 = h_8$ $P_9 = P(T_9, h_9)$ $s_9 = s(T_9, h_9)$	$\Delta h_{HX,max} = h_9 - h(T_9, P_4)$ $\Delta h_{HX} = h_3 - h_4$	

2.2.3 Solar PV Analysis: The PV power is calculated from the following equation

$$\dot{W}_{solar} = \eta_{PV} \times IT \times A \times \alpha \tag{12}$$

where IT is the total irradiation in W/m^2, α is the surface absorptivity, A is the solar panel area in m^2 which will be selected based on the requirements as clearly explained in Section 2.3, and η_{PV} is the efficiency of the solar panels and calculated as follows

$$\eta_{PV} = 0.553 - 0.001 T_p \tag{13}$$

Applying energy balance on the solar panel yields

$$\dot{W}_{solar} = IT \times A \times \alpha - \epsilon \times \sigma \times A \times \left(T_p^4 - T_o^4\right) - h \times A \times (T_p - T_o) \tag{14}$$

where ϵ is the emissivity, σ is the Stefan Boltzmann constant, T_p is the panel temperature, and T_o is the instantaneous air temperature at any time during the day in Kelvin. The solar time is found as follows (McQuiston et al., 2005)

$$\text{ST} = \text{Time} + \frac{[(L_S - L_L)\,\langle 4 \text{ min/deg}\rangle + \text{EOT}]}{60 \text{ min/hr}} \tag{15}$$

knowing that L_L and L_S are the longitude and standard longitude, respectively. EOT is the equation of time in minutes and is calculated as follows

$$\text{EOT} = 229.2\,[0.000075 + 0.001868\cos(N) - 0.032077\sin(N) - 0.014615\cos(2N) - 0.04089\sin(2N)] \tag{16}$$

where N is in (degrees) and obtained as follows

$$N = (\text{Day} - 1)(360/365) \tag{17}$$

Based on the solar time, the hour angle in degrees is calculated as follows

$$h^\circ = (\text{ST} - 12\ \langle\text{hour}\rangle) \times 15\ \langle\text{deg/hr}\rangle \tag{18}$$

Declination angle and angle of incidence in (degrees) are calculated from Equations 19 and 20, respectively

$$\delta = 23.45 \sin\left[360\left(\frac{284 + \text{Day}}{365}\right)\right] \tag{19}$$

$$\theta = \cos^{-1}[\sin(\delta)\sin(\varphi)\cos(\beta) - \sin(\delta)\cos(\varphi)\sin(\beta)\cos(\gamma) + \cos(\delta)\cos(\varphi)\cos(\beta)\cos(h^\circ) \cos(\delta)\sin(\varphi)\sin(\beta)\cos(\gamma)\cos(h^\circ) + \cos(\delta)\sin(\gamma)\sin(\beta)\sin(h^\circ)] \tag{20}$$

Note that φ is the latitude and γ is the surface azimuth angle, and it equals to the solar azimuth angle which can be evaluated as follows

$$\gamma = \gamma_s = \frac{h^\circ}{|h^\circ|}\left[\cos^{-1}\left(\frac{\cos(\theta_z)\sin(\varphi) - \sin(\delta)}{\sin(\theta_z)\cos(\varphi)}\right)\right] \tag{21}$$

β is the slope and it is equivalent to the solar zenith angle that is calculated as follows

$$\beta = \theta_z = \cos^{-1}[\cos(\varphi)\cos(\delta)\cos(h^\circ) + \sin(\varphi)\sin(\delta)] \tag{22}$$

The equation for the total irradiation is

$$IT = DNI\ \cos(\theta) + DIF\left(\frac{1+\cos(\beta)}{2}\right) + GHI\ \rho_g\left(\frac{1-\cos(\beta)}{2}\right) \tag{23}$$

where ρ_g is the ground reflectivity, *DNI*, *DIF*, and *GHI* are the normal direct, diffuse, and reflected irradiation, respectively, in W/m^2. The values of the last three parameters are measured at every hour for the average days of each hot month in Kuwait.

2.3 Assumptions and Design Conditions

The cooling capacity for an AC unit in typical resident in Kuwait is 5 tons of refrigeration ($\dot{Q}_{evap}$ = 17.6 kW). The outdoor temperatures (T_H) are the exact temperatures at specific times during the hot days in Kuwait. The indoor temperature (T_L) is the regular room temperature, which is 23°C. Also, it is assumed that the compressors have an isentropic efficiency of 80%. Other assumptions include:

- Negligible pressure drops across the components of the system.
- Subcooling temperature T_{sub} = 5°C, superheat temperature T_{sh} = 5°C, and pinch point temperature T_{pinch} = 5°C,
- Evaporator and condenser temperatures are: $T_{evap} = T_L - T_{sh} - T_{pinch}$, and $T_{cond} = T_H + T_{sc} + T_{pinch}$, respectively.
- Single-axis solar tracking panels to maximize the solar production by following the sun rays during the day.
- Other variables and Kuwait weather data required for the solar power calculations are listed in Table 3.

Table 3: Assumed parameters for Kuwait weather data required for the solar power calculations.

α = 0.83	ϵ= 0.9	ρ_g = 0.65	φ = 28.71°	L_L = 312.22°	L_S = 315°	$\sigma = 5.67 \times 10^{-8}$ W/m^2-K^4

3. RESULTS AND DISCUSSION

In this section, the main outcomes of this work are presented after solving all the previously defined equations using EES (Klein and Alvarado, 2019). Solving Equation 11 shows that a heat exchanger with an effectiveness of 0.82 is suitable for this work.

3.1 Optimal Refrigerant Selection

Different refrigerants were tested, and the optimum refrigerant, which is R-600, was chosen. The superiority of this refrigerant is shown in Figures 3 and 4. The improvement on the COP of the cycle shown in Figure 1 was checked for different working refrigerants, outdoor temperatures, and subcooling temperatures. In the beginning, two outdoor temperatures were examined, which are 35°C (representing the temperature during the moderate days in Kuwait) and 55°C (representing the temperature during the hot days in Kuwait). The tested refrigerants are R-410A, R-123yf, R-1234ze(E), R-32, R-290, R-600 and R-600a as mentioned previously. For both ambient temperatures and at different subcooling temperatures, R-600 showed better improvement on the COP of the cycle. In addition, R-600 is eco-friendly refrigerant because it has zero ODP and very low GWP. After that, the cycle performance was studied during the 24 hours of the day and during the hot months in Kuwait, namely, from May to September. This means that the outdoor temperature is varying with time, as clarified later. Figures 3 and 4 show that the best subcooling temperature, which gives the maximum improvement on the COP of the cycle for the moderate days, is 12°C, while 20°C is the optimum subcooling temperature degree for the hot days (*i.e.,* T_{amb} = 55°C). As the main goal of this work is to improve the performance of the refrigeration cycle during the extremely hot days in Kuwait, the second case is selected to be studied and analyzed in this work.

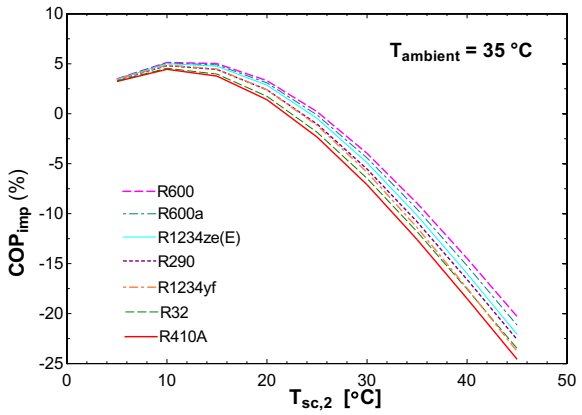

Figure 3: The system COP percentage improvement for different subcooling temperatures and various investigated refrigerants at outdoor temperature of 35°C.

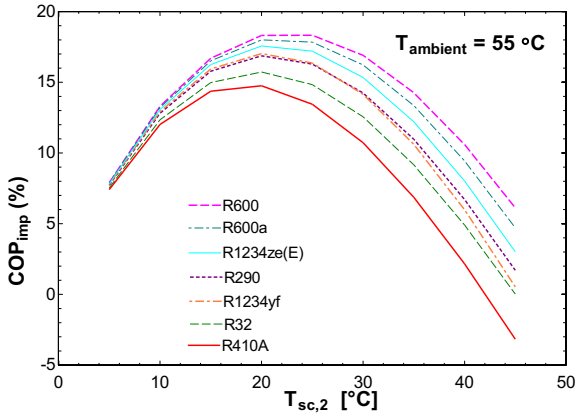

Figure 4: The system COP percentage improvement for different subcooling temperatures and various investigated refrigerants at outdoor temperature of 55°C.

3.2 Solar Power

The relation between solar power and time of the day is presented in Figure 5 for the average day of each hot month in Kuwait, namely, from May to September. The average day or in other words, the typical day for those months are the day number 135, 162, 198, 228, and 258, respectively (Duffie and Beckman, 2013). As it can be seen from Figure 5, the maximum solar power is produced in the middle of the day (*i.e.,* time = 12). The minimum solar power is produced during the month of September, while the maximum one is produced in the month of May. This is because the total irradiation produced at this time during the month of May is the highest. Overall, the solar power values obtained from the 3.9 m^2 solar panels on a hot day are close to the solar power values produced on the other hot days. The selection of this optimal area is explained in the next section.

3.3 Solar System Sizing

The solar panels used to run the system shown in Figure 1 are battery-operated. In this section, the number of batteries required are determined and explained to run the refrigeration system for 24 hours per day during the hot months in Kuwait. Before determining the required number of batteries, the area of the solar panels must be selected. The selection of the area of the solar panels is based on the following steps:

1. Defining the total work rate required for the dedicated mechanical solar-powered cycle.
2. The total work rate produced from the solar-powered cycle should be sufficient for the batteries to operate for 24 hours per day. To find the value of the total work rate in kWh, correlations of $\dot{W}_2$ and $\dot{W}_{solar}$ as functions of time were derived, and the areas under the curve were evaluated. This is clarified in Figure 5, where $\dot{W}_2$ and $\dot{W}_{solar}$ are plotted versus time for the hot months, and the enclosed area between the two curves for each month is calculated.
3. Each battery has a capacity power of 100 W, and hence for one day, the total power produced from each battery is 2.4 kWh. However, in this work, only 50 W is provided by each battery. This means that one battery provides a power of 1.2 kWh per day. Note that the battery power is selected based on the applicability and availability of this study.

From the above three points, the area of the solar panels was calculated and found to be equal to 3.9 m^2. This area should be sufficient for all hot months in Kuwait. In addition, the designed system needs eight batteries to satisfy the design requirement. For the connection of the batteries, it is recommended to have four batteries in series to get a total voltage of 48 V since each battery has a voltage of 12 V. The remaining batteries need to be connected in parallel with the series set connection. The reason for choosing such a connection is that typical applications use 48 V and to get a reasonable electric current that can pass through the 1.5 mm core cable that is commercially available. The connection of the batteries is represented in Figure 6.

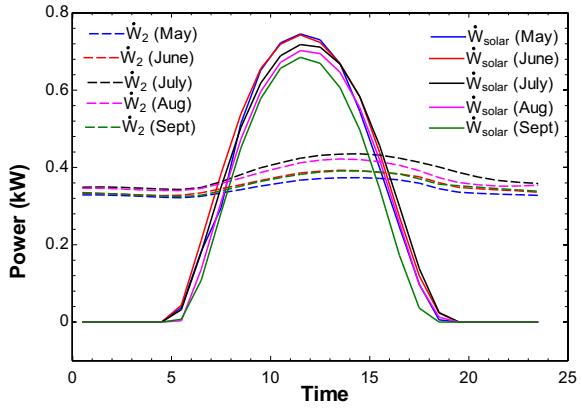

Figure 5: Subcooling cycle compressor power ($\dot{W}_2$) and solar power generation ($\dot{W}_{solar}$) versus time simulated for solar panel area of 3.9 m^2 for typical days during hot months in Kuwait.

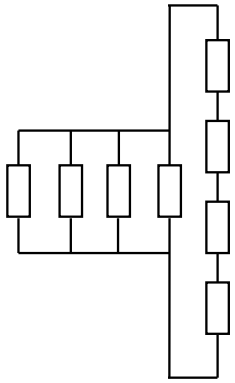

Figure 6: The proposed battery connections to optimize solar power generation.

3.4 Effect of Area on Power Demand

Figure 7 illustrates the effect of the solar panel area on the power demand during the month of August as an example. The results show that as the area increase, the solar power consumption increases as well. This happens because solar power is directly proportional to the area of the solar panels. However, the excess area results in excessive solar power that extremely exceeds the compressor power demand which means that a waste of energy occurs. Also, if the area results in a power that is less than the compressor power, the system will not be able to produce the required energy. Therefore, an area of 3.9 m^2 is sufficient for this work, yet no need to enlarge the solar panel size that might also increase the cost.

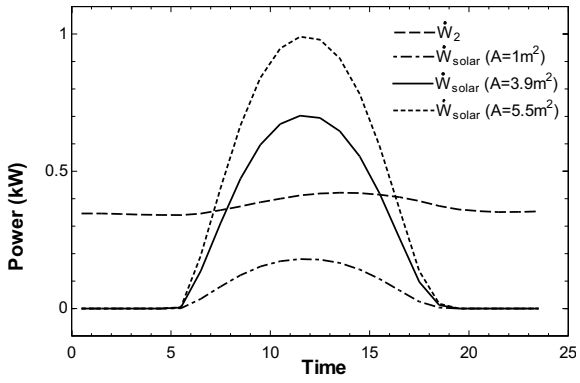

Figure 7: Effect of solar panel area on the power demand during the typical day of August.

3.5 Monthly COP Improvement

As it desired to improve the performance of the refrigeration system during the hot days in Kuwait using solar power, the relations between time and both COP of the proposed cycle and the baseline cycle and the improvement on COP were plotted versus time for the selected solar panel area of 3.9 m^2 and for the hot months in Kuwait as represented in Figures 8 and 9.

It can be noticed from Figure 8 that the combined system total COP is greater than the baseline COP during the 24 hours of each typical day of the hot months in Kuwait. From midnight to sunrise, the COP increases because the outside temperature decreases during this time; which results in better system performance. Then, the COP value decreases from sunrise up to approximately time = 15 (*i.e.,* 3:00 PM) due to the gradual increase in the outside temperature during this period of the day. After that, the COP starts to increase again as the outside temperature decreases during

nighttime. It can be noticed that the maximum COP values occur in May as it has the lowest outside temperatures among the studied months. On the other hand, the minimum COP values are associated with the month of July because July is the hottest month in Kuwait.

With respect to the improvement in system COP, Figure 9 shows that there is a considerable improvement in the system COP values during the 24 of each typical day of the hot months in Kuwait compared to the baseline case. From midnight to sunrise and from sunset to midnight, the improvement is relatively low compared to the improvement during the daytime because there is no solar power produced during these times which means that the combined cycle will benefit only from the extra subcooling. From sunrise up to the middle of the day, the improvement increases due to the increase in solar power values. This means that the combined cycle during the daytime can benefit from both subcooling and solar energy. From the middle of the day up to sunset, the improvement starts to decrease because of the decrement in solar energy. The maximum improvement occurs at the middle of the day because the largest solar power value is obtained at this time as mentioned earlier. A maximum improvement of approximately 16% can be achieved during the hottest month (*i.e.* during month of July)

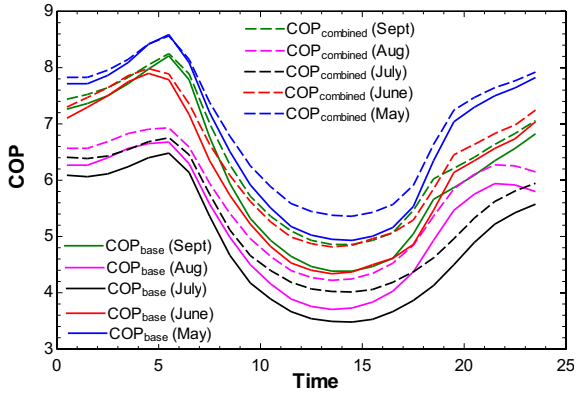

Figure 8: Baseline cycle and combined system total COP with time during typical days of each hot month in Kuwait.

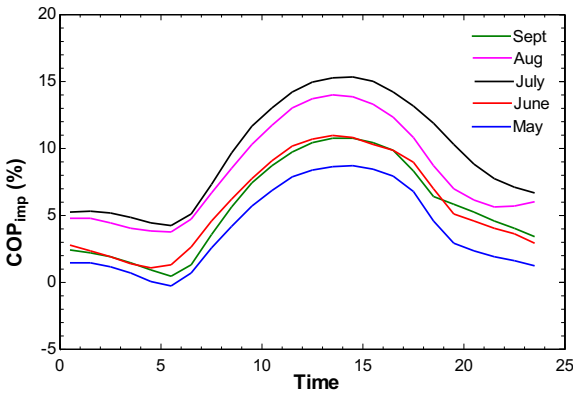

Figure 9: Percentage COP improvement with time during typical days of each hot month in Kuwait.

3.6 Utility Power Saved

The percentage of power saved by implementing the dedicated mechanical subcooling cycle during the 24 hours of each typical day was calculated and presented in Table 4. Table 4 shows that the proposed system can save up to approximately 10% of the utility power during the summer season in Kuwait. The maximum power saved is achieved during the typical day of July, which is the hottest month in Kuwait. This means that the proposed system fulfilled its objective by providing additional cooling in the hottest month using solar energy. On the other hand, the minimum power saved is associated with the typical day of May which is the coldest month compared to the months under investigation and during which the maximum solar power is produced.

Table 4: Percentage of utility power saved during typical days of each hot month in Kuwait.

Typical Day in	$\dot{W}_{base}$ (kWh)	$\dot{W}_{combined}$		$\dot{W}_{saved}$	
		$\dot{W}_{utility}$ (kWh)	$\dot{W}_{solar}$ (kWh)	Demand (%)	Total (%)
May	63.1	52.4	7.9	17.0	4.5
June	70.8	58.2	8.2	17.8	6.2
July	88.4	71.1	8.9	19.6	9.5
August	81.6	66.2	8.6	18.9	8.3
September	70.0	57.6	8.2	17.7	6.0

4. CONCLUSIONS

In this work, a solar-powered mechanical subcooling refrigeration system is introduced for hot climates. The proposed design is investigated for different subcooling temperatures, working refrigerants, and solar panel areas. The introduced system is tested for the hot months in Kuwait, namely, from May to September, during the 24 hours of each typical day of these months. The baseline cycle of the proposed system uses R-410A as a working fluid. The results obtained from this work show that the performance of the dedicated mechanical subcooling cycle can be maximized using R-600 refrigerant, which is eco-friendly with zero ODP and very low GWP. Also, it was found that the optimum subcooling temperature for the hot months in Kuwait is 20°C. Solar panels area of 3.9 m^2 is required to achieve the objective of this work as single-axis solar tracking panels are used which means that if fixed-slope panels were considered, larger area will be needed. For the months under investigation, the maximum solar power is produced in May. With respect to time, the maximum solar power occurs in the middle of the day, which results in total power saving between 5% to 10% and utility power-saving between 17% to 20%, during the typical day of the hottest month in Kuwait. The proposed solar-assisted refrigeration system shows excellent improvement in performance during the 24 hours of the day by up to approximately a 16% increase in COP during the typical day of July. In conclusion, the proposed dedicated mechanical subcooling cycle results in a better performance along with reducing utility power consumption by using the solar energy.

ACKNOWLEDGEMENT

The authors would like to acknowledge the support received from Kuwait University.

REFERENCES

Bahman, A. M., Groll, E. A., Horton, W. T., and Braun, J. E. (2014). Technologies to improve the performance of A/C systems in hot climate regions. In *15th International Refrigeration and Air Conditioning Conference at Purdue*, Paper 2284.

Bellos, E., Vrachopoulos, M. G., and Tzivanidis, C. (2017). Energetic and exergetic investigation of a novel solar assisted mechanical compression refrigeration system. *Energy Conversion and Management*, 147:1–18.

Duffie, J. A. and Beckman, W. A. (2013). *Solar Engineering of Thermal Processes, Photovoltaics and Wind*. John Wiley & Sons.

Klein, S. and Alvarado, F. (2019). Engineering equation solver, academic commercial version 10.644. *F-Chart Software, Madison, WI*.

Koronaki, I., Papoutsis, E., and Papaefthimiou, V. (2016). Thermodynamic modeling and exergy analysis of a solar adsorption cooling system with cooling tower in mediterranean conditions. *Applied Thermal Engineering*, 99:1027–1038.

Li, Z., Chen, E., Jing, Y., and Lv, S. (2017). Thermodynamic relationship of subcooling power and increase of cooling output in vapour compression chiller. *Energy Conversion and Management*, 149:254–262.

Li, Z., Yu, J., Chen, E., and Jing, Y. (2018). Off-design modeling and simulation of solar absorption-subcooled compression hybrid cooling system. *Applied Sciences*, 8(12):2612.

McQuiston, F. C., Parker, J. D., and Spitler, J. D. (2005). *Heating, ventilating, and air conditioning: analysis and design*. John Wiley & Sons.